The dependence of coercivity and corrosion resistance on grain size in Nd-Fe-B-type sintered permanent magnets

1991 J. Phys.: Condens. Matter 3 5893

(http://iopscience.iop.org/0953-8984/3/31/012)

J. Phys.: Condens. Matter 3 (1991) 5893–5901. Printed in the UK

The dependence of coercivity and corrosion resistance on grain size in Nd–Fe–B-type sintered permanent magnets

S Szymura†, H Bala‡, Yu M Rabinovich§, V V Sergeev§,
G Pawłowska‡ and D V Pokrovskii§

† Institute of Physics, Technical University, al. Armii Krajowej 19, 42-200 Częstochowa, Poland

‡ Institute of Chemistry, Technical University, al. Armii Krajowej 19, 42-200 Częstochowa, Poland

§ Department of Magnetic Materials, VNIIEM, GSP-6 Moscow, USSR

Received 31 January 1991, in final form 21 March 1991

Abstract. The microstructure, effect of grain size on the coercivity and corrosion behaviour of $Nd_{14}DyFe_{69.5}Co_5AlCr_2B_{7.5}$ sintered magnets have been investigated. Besides the hard magnetic boride phase $(Nd, Dy)_2(Fe, Co, Al, Cr)_{14}B$, a boron-rich phase $(Nd, Dy)_{1+\epsilon}(Fe, Co, Cr)_4B_4$ and non-magnetic Nd–Co phase (probably Nd_3Co) along grain boundaries were detected in sintered magnets. The coercivity and domain structures of the magnets with various mean grain size were analysed. It is shown that the coercivity decreases with increasing grain size and depends on the homogeneity of the distribution of the non-magnetic Nd-rich phase along grain boundaries. The corrosion resistance of the investigated magnets is also improved by the formation of a Nd–Co grain boundary phase, probably Nd_3Co and, generally, it increases with increasing mean grain size.

1. Introduction

The high coercive field in sintered RE–Fe–B magnets, as shown by direct observations [1], is determined by the nucleation of reversed domains and in real magnets is described theoretically by the sum of the effective nucleation field and the effective demagnetization field [2–7]:

$$H_c = (2K_1/\mu_0 M_s)\alpha_k \alpha_\psi - N_{eff} M_s. \tag{1}$$

Here K_1 denotes the first anisotropy constant, M_s is the spontaneous magnetization, N_{eff} is the effective demagnetization factor of the particles (non-magnetic grain and sharp edges produce large demagnetization fields), α_k gives the reduction in the ideal nucleation (coercive) field in regions with distributed material parameters (i.e. at the grain boundaries), and α_ψ describes the effect of grain orientation (i.e. it results from a certain averaging over the different nucleation fields for all grain orientations).

The parameters α_k, α_ψ and N_{eff} describing the microstructure in real sintered RE–Fe–B magnets seem to be in general a complicated function of the material parameters.

The important problem not yet solved is the effect of grain size of the magnetically hard phase $RE_2Fe_{14}B$ on the coercive field. So far this problem has not been satisfactorily

0953-8984/91/315893 + 09 $03.50

treated by theories of coercive field in sintered RE–Fe–B magnets [2–7]. However, it has been proved experimentally that the coercive field in this material decreases with increasing grain size within the range 3.5–7.5 μm [8–11].

By assuming in equation (1) a more general α-parameter ($\alpha = \alpha_k \alpha_\psi$) Hirosawa [11] has revealed that in a Pr–Fe–B magnet the grain size affects the reduction factor α, keeping the local demagnetization field coefficient N_{eff} unchanged.

A separate problem, although an important one from the application point of view, is the corrosion resistance of sintered RE–Fe–B magnets. It is known that these magnets are characterized by poor corrosion resistance which is due to fast oxidation of the B-rich and Nd-rich phases located around the grains of the hard magnetic $RE_2Fe_{14}B$ phase [12, 13]. So far, the effect of alloying additions has mainly been examined [14–19] whereas the effect of the grain size on corrosion resistance of these magnets has not yet been determined.

The purpose of our investigations is to find the reason for the effect of the grain size within the range 8.1–18.6 μm (i.e. the grain size occurring in industrial magnets) on the magnetic properties and corrosion resistance of sintered $Nd_{14}DyFe_{69.5}Co_5AlCr_2B_{7.5}$ permanent magnets.

2. Experimental details

The sintered $Nd_{14}DyFe_{69.5}Co_5AlCr_2B_{7.5}$ magnets used in this study were prepared as follows.

(i) Starting materials of 99.9% purity were used.

(ii) Powders of various grain sizes for sintered magnets were prepared by jet milling and classifying fractions using the Fisher subsieve size method.

(iii) The green compacts were aligned in a magnetic field of 16000 kA m^{-1} under a pressure of 200 MPa.

(iv) The green compacts were sintered at 1380 K for 2 h in an argon atmosphere and then cooled rapidly to room temperature.

(v) Annealing was carried out at temperatures of 930 K for 1 h and 870 K for 2 h.

After sintering, the mean grain sizes values of the samples were determined using a Quantimet method. These grain sizes for the tested samples varied from 8.1 to 18.6 μm.

The permanent magnet properties were measured by hysteresis graph with a maximum magnetized field of 2400 kA m^{-1}.

Metallography (optical and scanning microscopy) was employed to study the microstructures of the magnets. X-ray and electron diffraction techniques were used to determine the chemical compositions of the various phases.

Magnetic domain structures for planes parallel to the alignment axis were observed at room temperature by the powder pattern method.

To characterize the corrosion behaviour of the tested magnets the following corrosion tests were carried out:

(i) acid corrosion test: spontaneous dissolution of the tested magnet in a non-stirred 0.5 M H_2SO_4 solution deaerated with argon at 298 K;

(ii) potentiokinetic polarization curves: Ar-saturated solution of 0.5 M H_2SO_4, at 298 K with a disc rotation rate of 13 rev s^{-1} and a potential scanning rate of 0.1 V min^{-1}, starting with a cathodic potential φ of -1.3 V and increasing up to potentials close to $+2.3$ V (against a saturated calomel electrode (SCE));

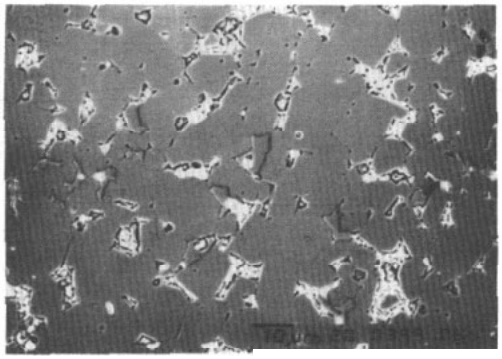

Figure 1. Back-scattered electron image of a sintered $Nd_{14}DyFe_{69.5}Co_5AlCr_2B_{7.5}$ permanent magnet. (Magnification, 500×.)

(iii) abnormal dissolution test: weight loss at strong cathodic polarization ($\varphi = -1.0$ V versus SCE; 0.5 M H_2SO_4 solution deaerated with argon at 298 K and 13 rev s^{-1});

(iv) accelerated atmospheric corrosion test in two environments: firstly an industrial consisting of exposure in humid (H_2O-saturated) air containing 3 mg SO_2 l^{-1} at 313 K and secondly an acetic acid salt spray (maritime) environment consisting of exposure in humid air passing through a solution containing 3% NaCl in 0.1 N CH_3COOH at a rate of 1.0 l h^{-1} at 313 K.

In corrosion tests, samples with three different mean grain sizes (8.1, 15.8 and 18.6 μm) were used.

The samples for the gravimetric tests were in the form of rectangular plates with an operating surface area S of 10 cm^2. The samples for electrochemical tests (polarization curves and abnormal dissolution) were rotating discs with $S = 0.10$ cm^2. Details of the apparatus and test method have been given in [20, 21].

3. Results and discussion

3.1. Microstructure and magnetic properties

A SEM micrograph of a sintered $Nd_{14}DyFe_{69.5}Co_5AlCr_2B_{7.5}$ magnet is shown in figure 1, and some exemplary microstructures of magnets of various grain size are shown in figures 2(*a*) and 2(*b*). Besides the hard magnetic $(Nd, Dy)_2(Fe, Co, Al, Cr)_{14}B$ phase (Φ), grains of the $(Nd, Dy)_{1+\epsilon}(Fe, Co, Cr)_4B_4$ phase (η) and intergranular $Nd_3(Fe, Co)$ phase (co) with only negligible amounts of Dy and Al are also detected in the intergranular phase. The formation of the non-magnetic co phase in Nd–Fe–Co–B alloys with an Al addition was also suggested by Yamamoto *et al* [22]. The Φ- and η-phases consist of exactly the same quantity of Cr, but the co phase is not Cr enriched. Moreover, along the grain boundaries, small globular and elongated precipitations of Fe–Cr occur, similar to what has been observed in [19].

It should also be noted that not all grain boundaries of the Φ-phase are isolated from each other and the probability of occurrence of such boundaries increases with increase in the grain size.

The variation in the coercive field, $\mu_0 H_c$ with the mean grain size $\bar{D}$ is shown in figure 2(*c*), where the results obtained in [8–10] are also shown for comparison. From figure

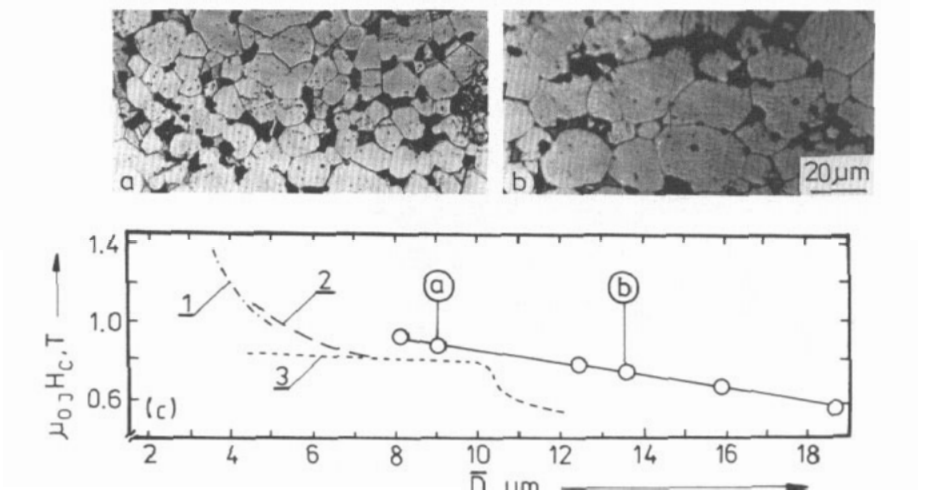

Figure 2. (*a*), (*b*) Optical micrographs of sintered $Nd_{14}DyFe_{69.5}Co_5AlCr_2B_{7.5}$ permanent magnets of mean grain size (*a*) 9.04 μm and (*b*) 13.57 μm. (*c*) Coercive field $\mu_0 J_c$ versus grain size $\bar{D}$: curve 1, $Nd_{15}Fe_{79}B_7$ [8]; curve 2, $Nd_{16}Fe_{78}Al_{0.5}$ [9]; curve 3, $Nd_{6.5}Fe_{18.5}$ [10].

2(*c*) it results that, within the entire range of grain sizes tested, the coercive field linearly decreases with increasing mean grain size.

The mean grain size of the hard magnetic Φ-phase in the sintered Nd–Fe–B magnets ranges between 3 and 20 μm, which is considerably more than the critical diameter for single-domain particles (0.26 μm) [23]. Consequently, these grains in the demagnetized state show domain patterns, as demonstrated in figures 3(*a*) and 3(*b*). In a few grains of magnets a coherent overlap of the domain pattern from one grain to the neighbouring grain is visible as indicated in figure 3(*a*) by arrows. With increasing grain size in the magnets, more and more grains which show such an overlap are present. An example of such a structure is presented in figure 3(*b*). The effect observed is connected with the presence or absence of a non-magnetic phase on the grain boundaries of Φ-phase. A layer of non-magnetic phase between the Φ grains may affect the magnetic decoupling of the exchange interaction between neighbouring Φ grains. This problem was also analysed by Adler and Hamann [24]. A moving domain wall disappears at the interface between the Φ and the non-ferromagnetic phase. At the surface of the neighbouring grain, a new domain wall must be formed with the aid of the stray field of the already remagnetized grain. Thus the non-magnetic phases act as a barrier against the remagnetization of succeeding grains. The degree of isolation of neighbouring Φ grains influences the parameter α in equation (1).

Real Φ-phase grains do not have a spherical shape but exhibit edges and corners which are the source of the local demagnetizing stray fields which increase with increasing grain size [25].

3.2. Corrosion tests

3.2.1. Acid corrosion test. The corrosion rates $v_{corr} = f(\tau)$ of the sintered $Nd_{14}DyFe_{69.5}Co_5AlCr_2B_{7.5}$ magnets with different mean grain sizes in 0.5 M H_2SO_4 solution are shown in figure 4. The SEM micrograph of this magnet after 8 min exposure

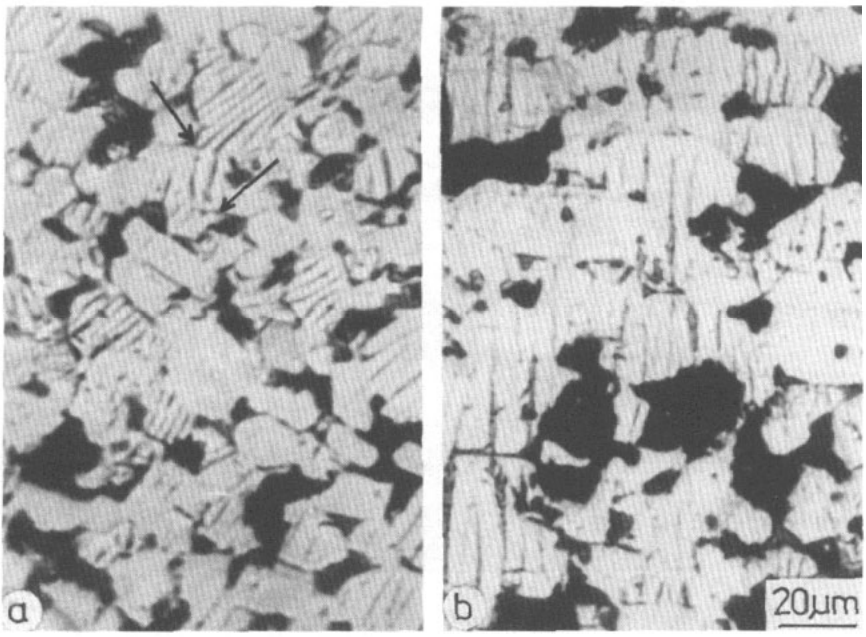

Figure 3. Domain structures of the thermally demagnetized sintered $Nd_{14}DyFe_{69.5}Co_5AlCr_2B_{7.5}$ permanent magnet for two mean grain sizes: (*a*) $\bar{D} = 15.9\,\mu m$; (*b*) $\bar{D} = 28.0\,\mu m$.

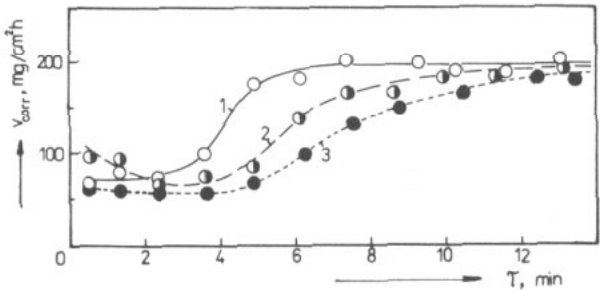

Figure 4. Kinetic curves of the etching of sintered $Nd_{14}DyFe_{69.5}Co_5AlCr_2B_{7.5}$ permanent magnets with a mean grain size 8.1 μm (curve 1) 15.8 μm (curve 2) and 18.6 μm (curve 3) in 0.5 M H_2SO_4 solution (298 K; no stirring).

in 0.5 M H_2SO_4 solution is illustrated in figure 5. From the shapes of the curves presented in figure 4 it can be seen that the initial corrosion rate in the acid solution decreases with increasing mean grain size, e.g. after $\tau = 3.5$ min, when v_{corr} tends to a minimum for samples with larger grain sizes, the corrosion rates are equal to 100 mg cm^{-2} h^{-1}, 70 mg cm^{-2} h^{-1} and 60 mg cm^{-2} h^{-1} for $\bar{D} = 8.1$ μm, 15.8 μm and 18.6 μm, respectively.

The evolution of the corrosion rate curves and micrographs coincides with the assumed mechanism of the corrosion of sintered RE–Fe–B-type magnets [12, 13] according to which the intergranular co phase is selectively dissolved together with the η-phase in the first stage of corrosion. The increase in grain refinement increases the fraction of co phase in the microstructure, which results in an increase in v_{corr}. The second stage of corrosion in which the grains of the Φ-phase are torn from the specimen surface is

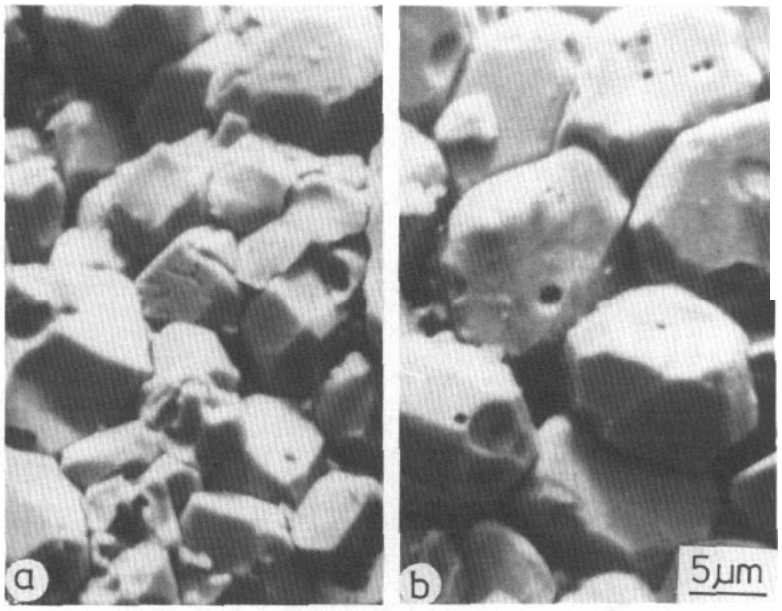

Figure 5. SEM micrographs of sintered $Nd_{14}DyFe_{69.5}Co_5AlCr_2B_{7.5}$ permanent magnets of various mean grain sizes after 8 min exposure in a 0.5 M H_2SO_4 solution (298 K; no stirring).

characterized by a constant corrosion rate and appears after a time which is dependent on the grain size. This time increases with increase in the mean grain size (see figure 4). After long etching times (12 min or more) the corrosion rate of the alloy tested is almost independent of grain size and for all specimens tested is $v_{corr} = 180$–190 mg cm^{-2} h^{-1}. For the magnet tested, this rate is nearly half that observed previously [17] for a $Nd_{15}Fe_{77}B_8$ magnet.

3.2.2. Atmospheric corrosion. The results of accelerated atmospheric corrosion tests of magnet are presented in figure 6. From the shapes of the curves obtained, it can be seen that in the 'industrial' environment (figure 6(*a*)) the corrosion behaviour of the magnet does not depend on the mean grain size, within the range of measurement error (±5%). In the more aggressive (from the corrosion point of view) environment of salt spray (figure 6(*b*)) the magnet of large mean grain size corrodes more slowly than do the magnets with small grains.

3.2.3. Polarization curves. In figure 7 the polarization curves of the magnets tested in deaerated 0.5 M H_2SO_4 solution are presented. As seen from the potentiokinetic polarization curves the mean grain size of the magnet almost does not affect their shape. Only in specimens with large grains, are a little higher values of cathodic and anodic currents observed in the vicinity of the cathodic potential, compared with the situation for specimens with smaller grains. At potentials $\varphi > 0.6$ V the alloys show a region of passive behaviour; however, the 'passive' currents, independent of the grain size, are of the order of 10–20 mA cm^{-2} (for pure iron these currents are about 0.1 mA cm^{-2} [18]). Therefore, we cannot speak about effective passivation of the samples tested although the tendency to passivation is stronger than that for base Nd–Fe–B magnet.

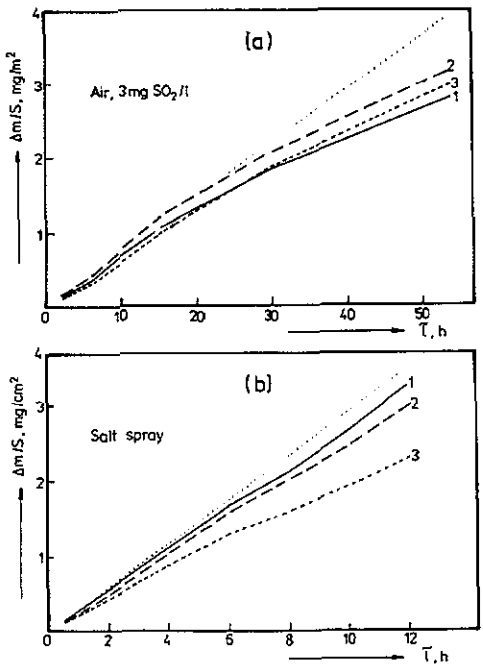

Figure 6. Mass increment (per 1 cm^2) of sintered $Nd_{14}DyFe_{69.5}Co_5AlCr_2B_{7.5}$ permanent magnets with a mean grain size of 8.1 μm (curves 1), 15.8 μm (curves 2) 18.6 μm (curves 3) in (*a*) industrial and (*b*) maritime environments as a function of exposure time (298 K): . . . . , $Nd_{15}Fe_{77}B_8$ (without addition).

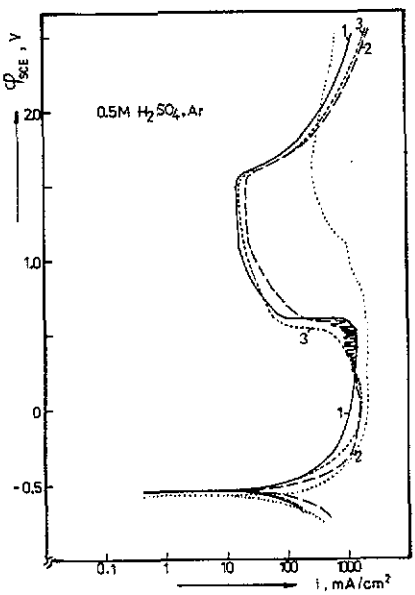

Figure 7. Potentiokinetic polarization curves of sintered $Nd_{14}DyFe_{69.5}Co_5AlCr_2B_{7.5}$ permanent magnets with a mean grain size of 8.1 μm (curve 1), 15.8 μm (curve 2) and 18.6 μm (curve 3) in Ar-saturated 0.5 M H_2SO_4 solution: . . . . , $Nd_{15}Fe_{77}B_8$ magnet.

Table 1. Corrosion rates of sintered $Nd_{14}DyFe_{69.5}Co_5AlCr_2B_{7.5}$ permanent magnets of various mean grain sizes at a cathodic potential $\varphi = -1.0$ V versus SCE (Ar; 0.5 M H_2SO_4; 13 rev s^{-1}; 298 K).

Mean grain size D (μm)	External cathodic current i_c (A cm^{-2})	Corrosion rate V_{corr} (mg cm^{-2} h^{-1})
8.1	2.0 ± 0.3	200 ± 20
15.8	1.4 ± 0.3	140 ± 15
18.6	1.6 ± 0.3	130 ± 10

3.2.4. Abnormal dissolution. The corrosion rates of the tested magnet with the different mean grain sizes measured at an external potential φ of -1.0 V versus SCE in 0.5 M H_2SO_4 solution are listed in table 1. From table 1 it can be seen that the increase in the mean grain size of the magnet almost does not influence the hydrogen evolution rate i_c;

however, it causes a slight decrease in the abnormal dissolution rate. Therefore, one can conclude that the increase in grain size inhibits the process of hydrogen uptake; this is obvious from the fact that RE–Fe–B magnets are able to absorb hydrogen easily owing to the reaction of the RE-rich intergranular phase with hydrogen [23, 26].

4. Conclusions

The results obtained in this paper show that in high-energy-density sintered $Nd_{14}DyFe_{69.5}Co_5AlCr_2B_{7.5}$ magnet the coercive field decreases with increasing mean grain size and the homogeneity of the distribution of the non-magnetic Nd-rich phase along grain boundaries can be correlated to the coercive field.

A small grain size is desirable to attain a high coercive field by

(i) better isolation of the hard magnetic Φ-phase,

(ii) decreasing the local demagnetization stray fields at the edges and at the corners and

(iii) reducing the probability of inhomogeneities at which demagnetization can be nucleated (if reversal of the magnetization starts, it is stopped earlier in small grains).

The corrosion resistance of $Nd_{14}DyFe_{69.5}Co_5AlCr_2B_{7.5}$ magnets increases with increasing grain size and this results from a smaller fraction of grain boundaries containing the Nd-rich phase in the microstructure.

The improvement in the corrosion resistance of the investigated magnets due to Co, Al and Cr addition has been attributed to

(i) formation of a Nd–Co grain boundary (probably Nd_3Co) phase which has replaced the Nd-rich grain boundary phase formed in magnets without Co and Al additions and

(ii) Cr enrichment of the η-phase.

Thus the compositional modification may alter the intergranular corrosion rate.

References

[1] Maki K, Forkl A, Dragon T and Kronmüller H 1989 *Phys. Status Solidi* a **116** 803
[2] Herzer G, Fernengel W and Adler E 1986 *J. Magn. Magn. Mater.* **58** 48
[3] Durst K H and Kronmüller H 1987 *J. Magn. Magn. Mater.* **68** 63
[4] Givord D, Tenaud P and Viadieu T 1988 *IEEE Trans. Magn.* **MAG-24** 1921
[5] Kronmüller H, Durst K D and Sagawa M 1988 *J. Magn. Magn. Mater.* **74** 291
[6] Sagawa M and Hirosawa S 1988 *J. Physique Coll.* **49** C8 617
[7] Kronmüller H, Durst K D, Hock S and Martinek G 1988 *J. Physique Coll.* **49** C8 623
[8] Ma B and Krause R F 1987 *Proc. 5th Int. Symp. on Magnetic Anisotropy and Coercivity in RE-Transition Metal Alloys* (*Bad Soden*) (Bad Honnef: Deutsche Physikalische Gesellshaft) p 141
[9] Müller K H, Eckert D E, Handstein A, Nothnagel P and Schneider J 1990 *J. Magn. Magn. Mater.* **83** 195
[10] Schneider G, Henig E-Th, Missell F P and Petzow G 1990 *Z. Metallk.* **81** 322
[11] Hirosawa S 1989 *IEEE Trans. Magn.* **MAG-25** 3437
[12] Sugimoto K, Sohma T, Minowa T and Honshima M 1987 *Japan Metals. Society Fall Meet.* (Tokyo: Japan Metals Society) p 604
[13] Bala H, Szymura S and Wysłocki J J 1990 *J. Mater. Sci.* **25** 571
[14] Ohashi K, Tawara Y, Yokoyama T and Kobayashi N 1987 *Proc. 9th Int. Workshop on RE–Magnets and Their Applications* (*Bad Soden*) (Bad Honnef: Deutsche Physikalische Gesellshaft) p 355
[15] Tenoud T, Vial F and Sagawa M 1989 *IEEE Trans. Magn.* **MAG-26** 1930
[16] Bala H, Szymura S and Wysłocki J J 1989 *IEEE Trans. Magn.* **MAG-26** 2645

[17] Bala H, Pawłowska G, Szymura S, Sergeev V V and Rabinovich Yu M 1990 *J. Magn. Magn. Mater.* **87** L255
[18] Bala H, Szymura S, Rabinovich Yu M, Sergeev V V, Pawłowska G and Pokrovskii 1990 *Rev. Phys. Appl.* **25** 1205
[19] Szymura S, Bala H, Rabinovich Yu M, Sergeev V V and Pawłowska G 1991 *J. Magn. Magn. Mater.* **94** 113
[20] Bala H and Przewłocka H 1981 *Corrosion* **37** 407
[21] Szymura S, Bala H and Gęga J 1989 *Mikrochim. Acta* **3** 43
[22] Yamamoto H, Hirosawa S, Fujimura S, Tokuhara K, Nagata H and Sagawa M 1987 *IEEE Trans. Magn.* **MAG-23** 2100
[23] Sagawa M, Fujimura S, Yamamoto H, Matsuura Y, Hirosawa S and Hiraga K 1985 *Proc. 4th Int. Symp. on Magnetic Anisotropy and Coercivity in RE–Transition Metal Alloys (Dayton, OH)* (Dayton, OH: University of Dayton) p 587
[24] Adler F and Hamann P 1985 *Proc. 4th Int Symp. on Magnetic Anisotropy and Coercivity in RE–Transition Metal Alloys (Dayton, OH)* (Dayton, OH: University of Dayton) p 747
[25] Blank R, Rodewald W and Schleede B 1989 *Proc. 10th Int. Symp. Workshop on Rare-Earth Magnets and their Applications (Kyoto)* p 353
[26] Bala H and Szymura S 1991 *Corros. Sci.* at press